CORA Cork Open Research Archive
Cartlann Taighde Oscailte Chorcaí

Title	Growth and characterization of anodic Films on InP in KOH and (NH4)2S
Authors	Harvey, E.;O'Dwyer, Colm;Melly, T.;Buckley, D. Noel;Cunnane, V. J.;Sutton, David;Newcomb, Simon B.
Publication date	2001-03-01
Original Citation	Harvey, E., O'Dwyer, C., Melly, T., Buckley, D. N., Cunnane, V. J., Sutton, D. and Newcomb, S. B. (2001) 'Growth and Characterization of Anodic Films on InP in KOH and (NH4)2S', III-Nitride Based Semiconductor Electronic and Optical Devices and State-of-the-Art Program on Compound Semiconductors XXXIV, 199th ECS Meeting, Washington, D.C., 25-30 March. in Proceedings - Electrochemical Society, Vol. 1, p. 204-212. ISBN 1-56677-306-5.
Type of publication	Conference item
Link to publisher's version	http://www.electrochem.org/199, http://ecsdl.org/site/misc/proceedings_volumes.xhtml
Rights	© 2001, Electrochemical Society
Download date	2026-11-16 11:47:02
Item downloaded from	https://hdl.handle.net/10468/2877



UCC
University College Cork, Ireland
Coláiste na hOllscoile Corcaigh

GROWTH AND CHARACTERIZATION OF ANODIC FILMS ON InP IN KOH AND $(NH_4)_2S$

E. Harvey[1], C. O'Dwyer[1,2], T. Melly[1,2], D.N. Buckley[1,2], V.J. Cunnane[2,3], D. Sutton[2], and S. B. Newcomb[2]

[1] Department of Physics, University of Limerick, Ireland
[2] Materials and Surface Science Institute, University of Limerick, Ireland
[3] Department of Chemistry and Environmental Science, University of Limerick, Ireland

ABSTRACT

The current-voltage characteristics of InP were investigated in $(NH_4)_2S$ and KOH electrolytes. In both solutions, the observation of current peaks in the cyclic voltammetric curves was attributed to the growth of passivating films. The relationship between the peak currents and the scan rates suggests that the film formation process is diffusion controlled in both cases. The film thickness required to inhibit current flow was found to be much lower on samples anodized in the sulphide solution. Focused ion beam (FIB) secondary electron images of the surface films show that film cracking of the type reported previously for films grown in $(NH_4)_2S$ is also observed for films grown in KOH. X-ray and electron diffraction measurements indicate the presence of In_2O_3 and $InPO_4$ in films grown in KOH and In_2S_3 in films grown in $(NH_4)_2S$.

INTRODUCTION

Under certain conditions, GaAs, InP and GaP have been made porous by anodization [1-3]. Investigations of the properties of these porous semiconductors has revealed that their photoluminescence spectra are significantly different than the luminescent properties exhibited by the bulk material. An interesting finding is the emission of visible radiation from both porous GaAs and GaP [4,5]. However the mechanism of this luminescence is not fully understood. It is not clear whether it is due to quantum confinement in the pores or is a property of surface oxides formed during anodization. Furthermore, anodically grown films formed on InP and GaAs in sulphur containing solutions have been reported to improve the electronic properties of these semiconductor surfaces [6,7]. Current oscillations during anodization have long been known to be a feature of silicon in fluoride-containing electrolytes [8,9] and have also been observed recently for InP in a sulphide electrolyte [10]. Such features have renewed interest in the localized dissolution and film formation processes on III-V semiconductors by anodization methods. Little work has been concentrated on the mechanisms that lead to pore formation, film growth and fluctuations in the current. In this paper we relate the current-voltage behavior to the physical features observed when n-InP is anodized in a KOH or $(NH_4)_2S$ electrolyte.

EXPERIMENTAL

InP (100) wafers were n-type with a carrier concentrations of ~10^{18} cm^{-3}. The electrolyte used was either 3 mol dm^{-3} aqueous $(NH_4)_2S$ or 5 mol dm^{-3} KOH. Ohmic contact was made by alloying In to the InP sample. The electrical contact was insulated from the electrolyte by coating with a varnish. All potentials were referenced to the saturated calomel electrode (SCE). Experiments were carried out at room temperature and in the dark.

For cyclic voltammetric measurements, a CH Instruments Model 650A Electrochemical Workstation was employed for cell parameter control and for data acquisition. Surface topography was examined by atomic force microscopy (AFM), scanning electron microscopy (SEM), optical microscopy and focused ion beam secondary electron microscopy (FIB). Transmission electron microscopy (TEM) electron diffraction and x-ray diffraction (XRD) were used to identify the structure of the anodic films.

RESULTS AND DISCUSSION

Fig 1. shows cyclic voltammetric measurements of an InP electrode in a KOH electrolyte. The potential was scanned at a rate of 2.5 mV s^{-1} between an initial value, E_i, of 0.0 V and upper potentials, E_u, of 0.665 V and 1.1 V respectively.

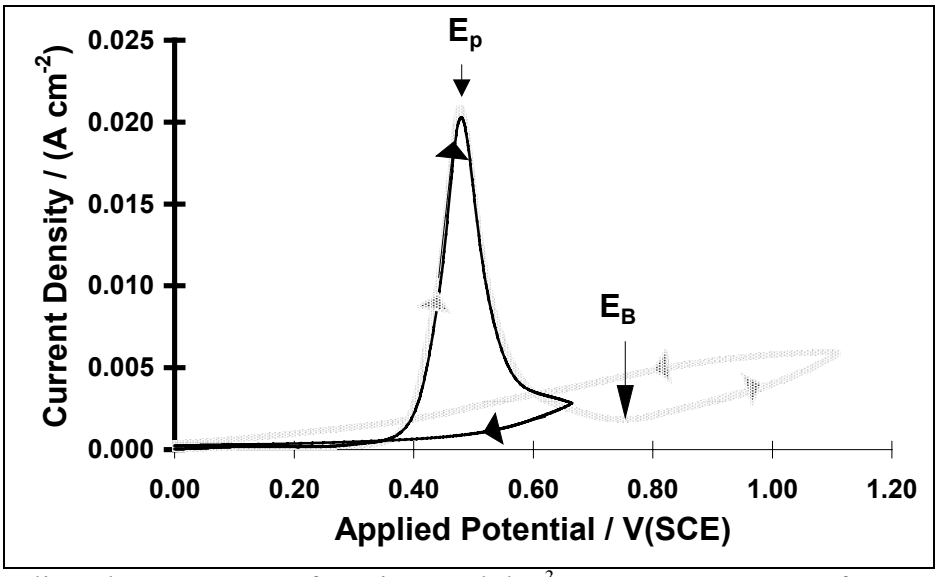


Fig.1 Cyclic voltammograms of InP in 5 mol dm^{-3} KOH at a scan rate of 2.5 mV s^{-1}. E_i = 0.0 V(SCE); (a) ——— E_U = 0.665 V(SCE) and (b) ——— E_U = 1.1 V(SCE)

On the forward scan a current peak can be observed at a potential E_P = 0.48 V, and following this peak the current drops to a very low value and reaches a minimum

current at ~0.75 V, termed E_B. If $E_U < E_B$ then the current on the cathodic scan remains very low as can be seen in Fig. 1(a). Such behavior is indicative of the formation of a blocking film which inhibits current flow and hence further film formation. For potentials greater than E_B, a slow rise in the current with increasing potential is observed. Fig. 1(b) shows that for $E_U > E_B$ the current on the reverse scan is slightly higher than the corresponding current on the forward scan (excepting the peak at E_P). As E_U is increased even further above E_B, the current on the reverse scan becomes more pronounced. This suggests that at potentials greater than E_B, further film growth occurs and this may be facilitated by porosity in the film. At potentials greater than 1.6 V there is a more rapid rise in the current, as shown in Fig. 2(b).

Cyclic voltammetric measurements were also carried out in an $(NH_4)_2S$ solution at a scan rate of 10 mV s^{-1}. A peak in current is observed on the forward scan at a potential E_P and a current minimum is reached at a potential E_{MIN}. Following this, there is a rise in current leading to a plateau region which continues to a potential E_B where the current rises sharply. A series of AFM images was taken as the value of E_U was increased. The images obtained suggest that, following the small peak on the forward scan, film growth continues up to and during the plateau region. When $E_P < E_U < E_B$, the current on the reverse scan is reduced over most of the potential range.

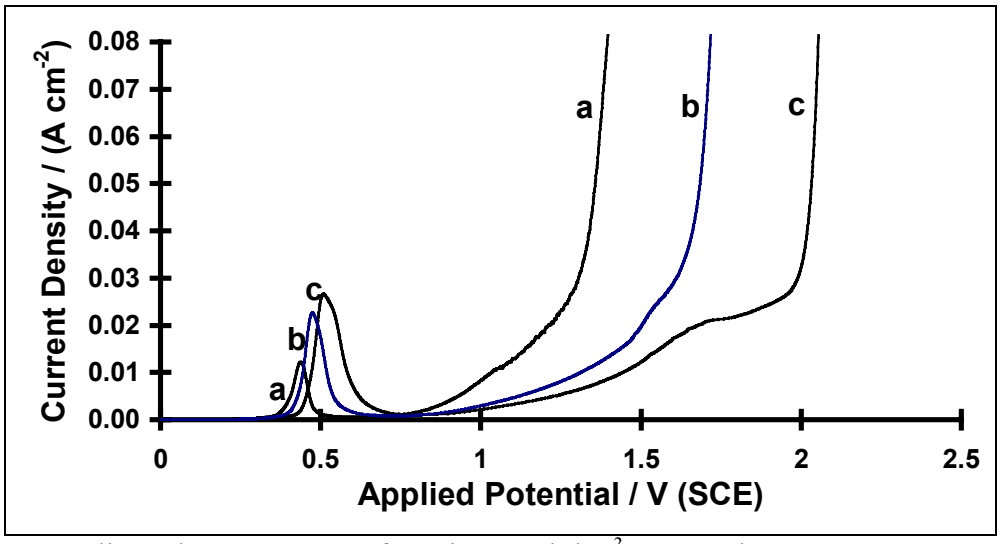


Fig. 2 Cyclic Voltammograms of InP in 5 mol dm^{-3} KOH. The sweep rates were (a) 1 mV s^{-1} (b) 2.5 mV s^{-1} and (c) 3.75 mV s^{-1}.

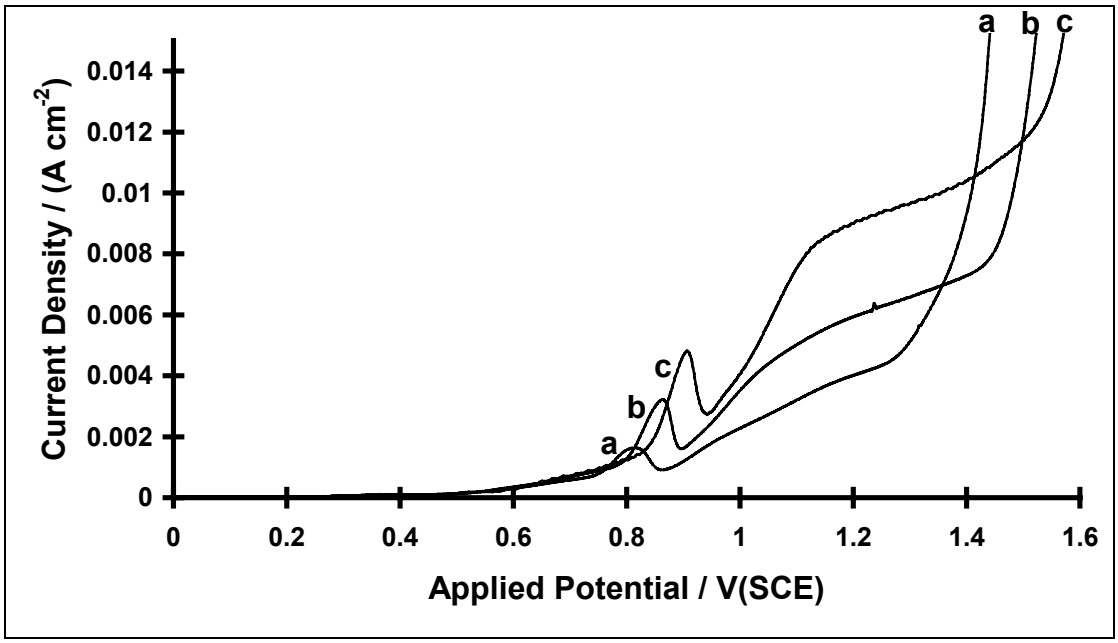


Fig. 3 Cyclic Voltammograms of InP in 3 mol dm^{-3} $(NH_4)_2S$. The sweep rates were (a) 5 mV s^{-1} (b) 10 mV s^{-1} and (c) 20 mV s^{-1}.

A series of cyclic voltammograms were carried out in both KOH and $(NH_4)_2S$ electrolytes, in which the scan rate was varied. Fig. 2 shows the forward scans obtained in the KOH electrolyte for scan rates of 1 mV s^{-1}, 2.5 mV s^{-1} and 3.75 mV s^{-1} respectively. As the scan rate was increased the value of E_B was found to shift to higher potentials. The characteristics of the cyclic voltammetric curves at these scan rates depended on E_U in a manner similar to that described for Fig. 1 above. At scan rates above 5 mV s^{-1} the passivation peak at E_P was replaced by two overlapping peaks. Voltammograms obtained in the $(NH_4)_2S$ electrolyte are shown in Fig. 3 for scan rates of 5 mV s^{-1}, 10 mV s^{-1} and 20 mV s^{-1} respectively. E_B was found to shift to more anodic values of potential with increasing scan rate. The current voltage characteristics were again found to be dependent on E_U in a manner similar to that described above for a 10 mV s^{1} scan rate in $(NH_4)_2S$. Scan rates between 5 mV s^{-1} and 1 V s^{-1} were investigated and it was observed that the current-voltage curves have a similar form to each other over this range.

The total charge corresponding to the peak at E_P was obtained by integrating the area under the curve (from 0.0 V to E_B). This charge was estimated for scan rates between 0.5 mV s^{-1} and 3.75 mV s^{-1} in the KOH electrolyte and was found to be constant. Thus the thickness of the passivating film, which is responsible for a drop in current, is independent of scan rate. A similar result is found for the peak at E_P in the films grown in the $(NH_4)_2S$ solution for scan rates between 5 mV s^{-1} and 1 V s^{-1} (integrated from 0.0 V to E_{MIN}).

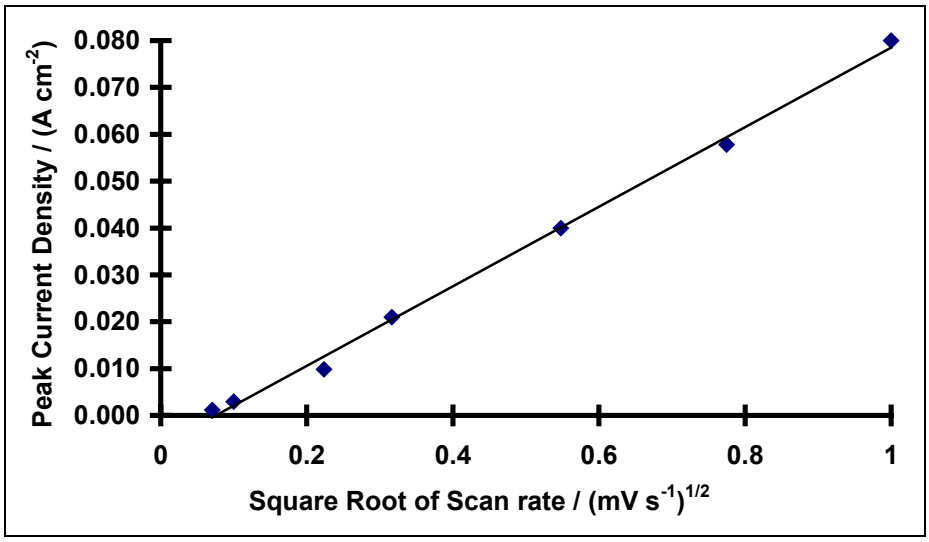


Fig. 4 Peak current plotted against square root of the scan rate for InP in a 3 mol dm^{-3} $(NH_4)_2S$ solution at scan rates from 5 mV s^{-1} to 1 V s^{-1}.

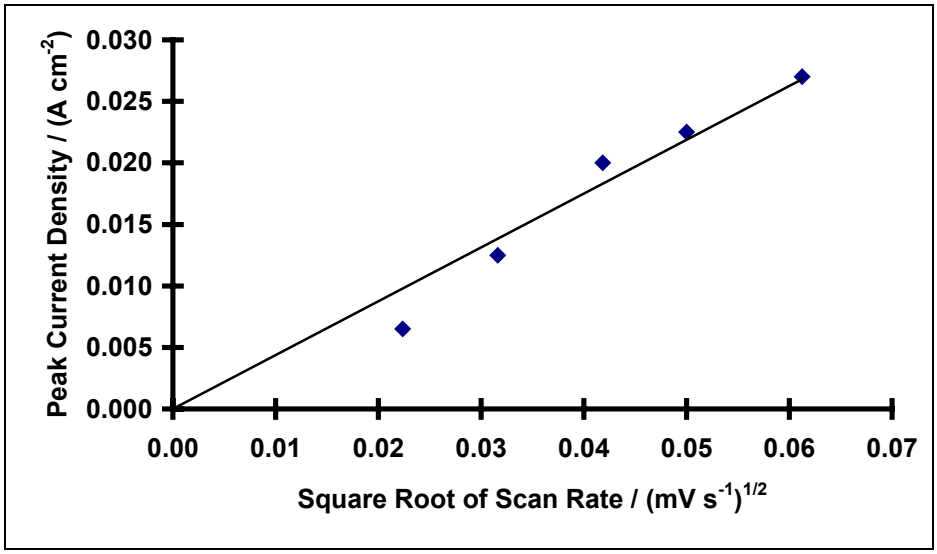


Fig. 5 Peak current plotted against the square root of the scan rate in a 5 mol dm^{-3} KOH solution at scan rates from 0.5 mV s^{-1} to 3.75 mV s^{-1}.

Data obtained from the potential sweep curves was also used to investigate the relationship between the peak current and the scan rate. For both the $(NH_4)_2S$ and the KOH solutions, a linear relationship was found between the peak current and the square root of the scan rate. This relationship is shown in Fig. 4 for the $(NH_4)_2S$ system and Fig. 5 for the KOH system. The peak current density is approximately proportional to the scan rate indicating that in both cases the film formation process appears to be diffusion controlled.

Thus the cyclic voltammograms suggest that the films formed in the KOH electrolyte at scan rates of less than 5 mV s^{-1}, and for $E_P < E_U < E_B$ are consistent with compact passivating films. Despite the fact that these films are formed at low scan rates, the current and potential values measured are very sensitive to the actual value of the scan rate and vary significantly even in the small range considered here. A passivating film is also formed on InP in the $(NH_4)_2S$ electrolyte but the passivation effect, as measured by the fractional decrease in current, is not as dramatic as in the KOH. However, the passivation effect occurs at a much lower film thickness, and subsequent growth leads to a less compact film. Indeed SEM micrographs of the cross section of the films grown in this region of potential reveal that the film has a columnar type structure. The current-voltage curves, which are indicative of the film growth behavior, have a similar form for a large range of scan rates in the $(NH_4)_2S$ solution. This indicates that the dynamic nature of the experiment does not change the formation processes significantly.

When $E_U > E_B$ in a cyclic voltammogram in the $(NH_4)_2S$ electrolyte, the current on the reverse scan was found to be considerably greater than the corresponding current on the anodic scan. In the KOH solution a similar effect was noted.

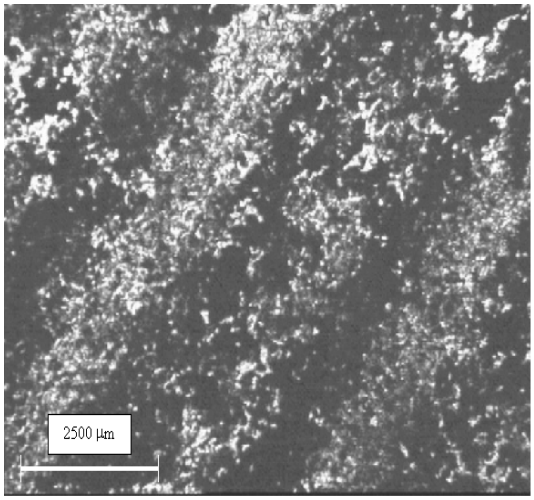


Fig. 6 Optical micrograph showing the film surface after a potential sweep experiment to $E_U > E_B$ in a 5 mol dm^{-3} KOH solution.

Optical microscopy was used to examine the nature of the film formed on an InP electrode anodized to $E_U > E_B$ in a 5 mol dm^{-3} KOH solution. An optical micrograph of the film surface is shown in Fig. 6. Under these conditions the film showed a periodic pattern across the area of the sample. These films were also examined in cross section and it was observed that the 'white' striped regions (A) correspond to a thinner film and the 'black' striped regions (B) to a thicker film. FIB microscopy was used to examine these regions of the films in further detail.

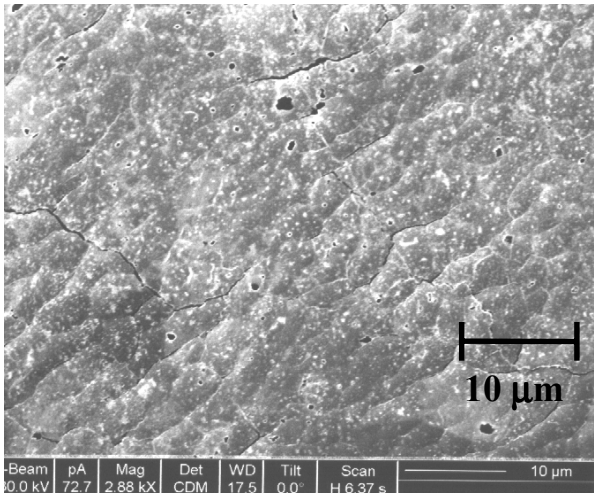


Fig. 7(a) FIB secondary electron image of the surface of the A region of the film formed in KOH for $E_U > E_B$

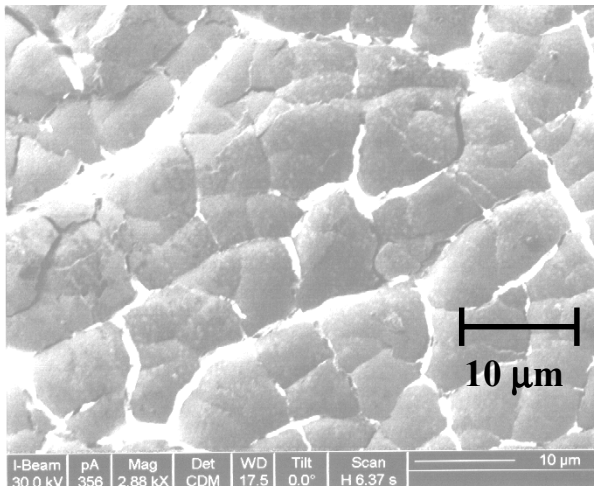


Fig. 7(b) FIB secondary electron image of the surface of the B region of the film formed in KOH for $E_U > E_B$

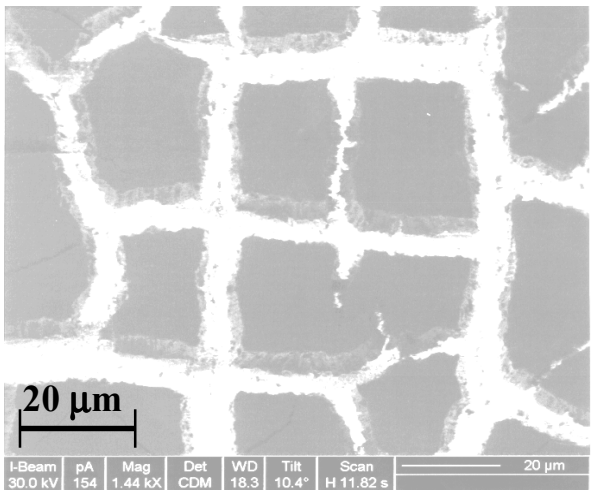


Fig. 7(c) FIB secondary electron image of the surface of the film formed in $(NH_4)_2S$ for $E_U > E_B$

The FIB image shown in Fig. 7(a) is of an A region and the film can be seen to have a nodular appearance. Fig 7(b) shows a FIB micrograph of a B region, and in this case a clear pattern of cracking can be observed. In comparison Fig. 7(c) shows a FIB image of the film formed after a potential sweep in the $(NH_4)_2S$ solution to $E_U > E_B$. It is obvious that on this scale the structure of the film formed in the $(NH_4)_2S$ electrolyte strongly resembles the B regions of the film formed in the KOH electrolyte. The cracked film formed in the $(NH_4)_2S$ electrolyte [10,11] was previously shown to result from shrinkage of the film as it dries [10]. It appears that the cracking occurs due to stress induced by drying of the highly porous film and does not necessarily imply stress in the wet film as grown; it is reasonable to postulate a similar mechanism in KOH.

Electron diffraction was used to determine the structure of the films formed under conditions of $E_U > E_B$. Analysis of the ring patterns obtained from the film formed in the $(NH_4)_2S$ solution indicates an In_2S_3 phase. The electron diffraction pattern for the film grown in the KOH solution indicates that both In_2O_3 and $InPO_4$ are present. XRD measurements also showed peaks corresponding to In_2O_3 and $InPO_4$.

CONCLUSIONS

The current-voltage behavior of InP electrodes, in both $(NH_4)_2S$ and KOH electrolytes indicates that passivating films are formed in both solutions. However, the initial passivation effect occurs for a much lower film thickness in the sulphide electrolyte. Peak currents are observed to be approximately proportional to the square root of the scan rate, indicating diffusion-controlled film growth. Film cracking of the type reported previously for films grown in $(NH_4)_2S$ is also observed for films grown in KOH. Electron diffraction and XRD results show the presence of In_2O_3 and $InPO_4$ in films grown in KOH and In_2S_3 in films grown in $(NH_4)_2S$.

REFERENCES

(1) G. Oskam, A. Natarajan, P. C. Searson, and F. M. Ross, *Appl. Surf. Sci.*, **119**, 160 (1997)

(2) S. Langa, I. M. Tiginyanu, J. Cartensen, M. Christophersen, and H. Foll, *Electrochem. Solid-State Lett.,* **3**, 514 (2000)

(3) B. H. Erne, D. Vanmaekelbergh, and J. J. Kelly, *J. Electrochem. Soc.*, **143**, 305 (1996)

(4) P. Schmuki, D. J. Lockwood, H. J. Labbe, and J. W. Fraser, *Appl. Phys. Lett.*, **69**, 1620 (1996)

(5) A. Anedda, A. Serpi, V. A. Tiginyanu, and V. M. Ichizli, *Appl. Phys. Lett.*, **67**, 3316 (1995)

(6) I. K. Han, D. H. Woo, H. J. Kim, E. K. Kim, J. I. Lee, S. H. Kim, K. N. Kang, H. Lim, and H. L. Park, *J. Appl. Phys*., **80**, 4052 (1996)

(7) Z. Chen, W. Kim, A. Salvado, S. N. Mohammed, O. Aktas and H. Morkoc, *J. Appl. Phys.*, **78**, 3920 (1995)
(8) H. Gerischer and M. Lubke, *Ber. Bunsenges. Chem.*, **92**, 573 (1988)
(9) J. N. Chazalviel, and F. Ozanam*, J. Electroanal. Chem.*, **327**, 343 (1992)
(10) E. Harvey and D.N. Buckley, in *Proceedings of the 32nd State-of-the-Art Program on Compound Semiconductors*, R.F. Kopf, A.G. Baca and S.N.G. Chu, Editors, PV 2000-1, p. 265, The Electrochemical Society, Proceedings Series, Pennington, NJ (2000).
(11) L.J. Gao, J. A. Bardwell, Z-H. Lu, M.J. Graham and P.R. Norton, *J. Electrochem. Soc.*, **142**, L14 (1995)